Prediction of Formation of Wavy Surfaces in Rolled Plates by Post-Buckling Analysis

Jinseok Kim
Department of Mechanical Engineering,
Pohang Institute of Science and Technology,
Pohang 790-784, Korea

Shrikant Pattnaik[1]
e-mail: mailspp@gmail.com

Jay Kim

Department of Mechanical Engineering,
University of Cincinnati,
Cincinnati, OH 45221-0072

Excessive wavy surfaces formed by a cold- or hot-rolling process in a thin plate degrades the value of the plate significantly, which is called the flatness problem in the industry. It is a result of post-buckling due to the residual stress caused by the rolling process. Because the buckling occurs in a very long, continuous plate, a unique difficulty of the problem as a buckling problem is that the buckling length is not given but has to be found. In many previous works, the length that gives the lowest critical load of the plate for the given load profile was taken as the buckling length. In this work, it is shown that this approach is flawed, and a new approach is developed to solve the flatness problem by extending a classic post-buckling analysis method based on the energy principle. The approach determines the buckling length and amplitude without using any unfounded assumptions or hypothesis. Using simple displacement functions, approximate solutions are obtained in closed forms for the plate subjected to a linearly distributed residual stress. The new solution approach can be used to determine the condition for the maximum rolling production that does not cause the flatness problem.
[DOI: 10.1115/1.4000908]

1 Introduction

In a thin metal plate produced by a rolling process, sometimes, excessively wavy surfaces are formed because of high residual stresses in the plate [1,2]. This is called the *wave* or flatness problem in the industry, which significantly diminishes the commercial value of the plate. Once formed, rectifying the problem using measures such as roller-leveling or edge-trimming is not only costly, but also ineffective. A much desired solution is preventing the problem by a proper design of the process, which requires an accurate simulation method to predict formation of the wave. The problem requires solving a post-buckling analysis. A unique difficulty of the problem is that the buckling length is not given, but has to be found because the wave is formed in a very long and continuous plate.

Various methods were proposed to predict the formation of the buckling wave, including empirical [3], analytical, or numerical methods [4–8]. A two-step approach has been employed in most of these numerical works. In the first step of the method, the buckling length is determined based on a prebuckling analysis. The plate length that gives the lowest critical load for the given load profile is selected as the buckling length. In the second step, the buckling amplitude is calculated by a post-buckling analysis for the buckling length of the plate found in the first step. However, the critical load decreases monotonically as a function of the plate length in many load cases. Obviously, the minimum critical load cannot be defined in these cases. Even if the minimum critical load is defined, the approach seems to find a buckling length, much longer than what is observed in actual products. It will be shown that the approach is actually based on a flawed interpretation of the wave formation process; therefore, it is incorrect.

Timoshenko and Gere [9] showed that an energy approach can be used to solve post-buckling problems. They found the deflection of the plate from the condition that minimizes the strain energy of the plate. It was realized by the authors that the method can be extended to determine the buckling length, that is, the buckling length can be determined from the condition to make the strain energy minimum for the entire rolled plate. The approach enables solving this type of post-buckling problem for the first time correctly without using any unfounded assumptions or hypotheses.

2 Preliminary Discussions

2.1 Definitions. Figure 1(*a*) illustrates a buckling wave formed in a very long rolled plate. Flatness, $\lambda = \delta/L$, the ratio of the buckling amplitude δ and buckling length L, is used in the industry to assess the seriousness of the problem. In this paper, the *plate length* indicates the natural length of the plate, and the *buckling length* indicates half of the wavelength of the wave formed in the plate. In most cases in plate buckling problems, the length of the plate is given and the critical load (in prebuckling problems) or the buckling amplitude (in post-buckling problems) is to be found. However, the buckling length is not given, but has to be found in the *wave* problem.

Due to the periodicity of the deformation, only one section of the plate shown in Fig. 1(*a*) can be used to represent the entire system. The section is shown as a free body in Fig. 1(*b*), which is a rectangular plate that has simply supported edges along the line $x=0$ and L, and free edges along the line $y=B$. The simply supported edges are subjected to the axial force. Only a symmetric, linearly distributed, self-equilibrated axial force is considered in this work. A more general form of axial load requires a numerical procedure, which is the subject of a sequel paper of this work.

Figure 1(*b*) shows that the axial force is compressive at the edge of the plate and tensile at the center of the plate, which is called the *edge compression* case. The *center compression* case refers to the opposite, the plate subjected to the axial force compressive at the center of the plate, and the tensile at the edge of the plate. The analysis method will be developed for the edge compression case, which can be easily modified to the center compression case. The edge load is the resultant of residual stresses resulting from the rolling process, which has to be calculated by a plasticity analysis of the rolling process [10].

Because of the symmetry of the system, only the upper half of the plate can be considered. The edge load $N_x(y)$ is represented as

[1]Corresponding author.

Contributed by the Applied Mechanics Division of ASME for publication in the JOURNAL OF APPLIED MECHANICS. Manuscript received November 21, 2008; final manuscript received October 19, 2009; published online April 9, 2010. Assoc. Editor: Jian Cao.

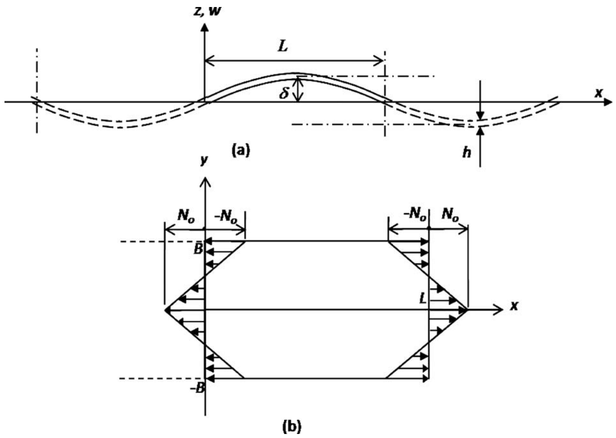

Fig. 1 Buckling wave formed in a rolled plate; (*a*) a very long plate where the wave is formed. Definitions of the buckling length (*L*), buckling amplitude (*δ*) and plate thickness (*h*) are shown. (*b*) The free body diagram of the plate section of one buckling length. Coordinate system and the edge load $N_x(y)$ are shown.

$$N_x(y) = N_0 n(y) = N_0\left(1 - 2\left(\frac{y}{B}\right)\right), \quad 0 \le y \le B \tag{1}$$

where N_0 is the maximum compressive load and $n(y)$ represents the load profile.

A prebuckling analysis can be conducted with the following assumed displacement field:

$$w(x,y) = W(y)\sin\frac{\pi x}{L} = (C_0 + C_1 y + C_2 y^2 + C_3 y^3 + \ldots)\sin\frac{\pi x}{L} \tag{2}$$

The prebuckling analysis is straightforward. For example, applying a Rayleigh–Ritz method leads to an eigenvalue problem in terms of N_0, and the smallest eigenvalue becomes the critical load [9,11].

2.2 The Flaw in the Past Approach That Used the Plate Length That Gives the Lowest Critical Load as the Buckling Length. Many researchers adopted an approach to use the plate length that gives the minimum critical load as the buckling length [5,6]. The buckling length determined as such is then used in the post-buckling analysis to calculate the buckling amplitude.

Figure 2 illustrates the implied logic of the aforementioned approach. The curve indicated as $N_{0,\mathrm{cr}}$ in Fig. 2(*a*) shows the critical load calculated for a given axial load profile as a function of the plate length. In this case, the buckling length will be determined as L_1, the plate length that gives the lowest critical load. This approach assumes that the axial load increases from a very small value (indicated as "*a*" in Fig. 2(*b*)) in a very long, initially *unstressed* plate to the level of the lowest critical load indicated as "*b*." In this case, the plate will deflect along the path *b-c* with the buckling length L_1, and buckling with other plate lengths will have no chance to occur.

While the logic explained above may appear plausible, however, for many edge load profiles, including the linear edge load in Fig. 1, the critical load decreases monotonically as a function of the plate length. Obviously, the *minimum* buckling load will not be defined; therefore, the buckling length will not be defined by the approach in these cases. Even for the cases in that the minimum buckling load is defined, the buckling length is often identified much longer than typical lengths observed in rolled plates. Also, the approach predicts that the wavelength will be independent of the magnitude of the edge load, which also contradicts with observations. This is because the approach is flawed. The flaw in the approach is explained as follows.

In the approach, it is assumed that the edge force of a very long plate starts to increase from a small value. In reality, the residual stress in the plate is quite high already when the plate exits the rollers. As it is illustrated in Fig. 3, the plate will exit the rollers in a unbuckled form with quite a high axial load. The length of this unbuckled part L (see Fig. 3) will keep increasing as the plate is rolled out, while the residual stress will also change. This process is described by paths 1–2 shown in Fig. 2(*a*). The plate will start to buckle when the unbuckled length L (the flat part before the wave is formed shown in Fig. 3) of the plate becomes L_c, long enough to initiate buckling of the plate. Note that at the end of path 1–2, the load N0 has to be higher than the critical load corresponding to L_c to cause an appreciable post-buckling deflection. From Fig. 2, it is easy to see that the buckling length will be completely different from what will be predicted by the minimum critical load hypothesis. Because it is not possible to find actual paths 1–2, we need to develop a new method to determine the buckling length. We develop the method based on the energy principle, as it will be discussed in Sec. 2.3.

2.3 Post-buckling Analysis Based on the Energy Principle. We reviewed the post-buckling analysis method used by Timosh-

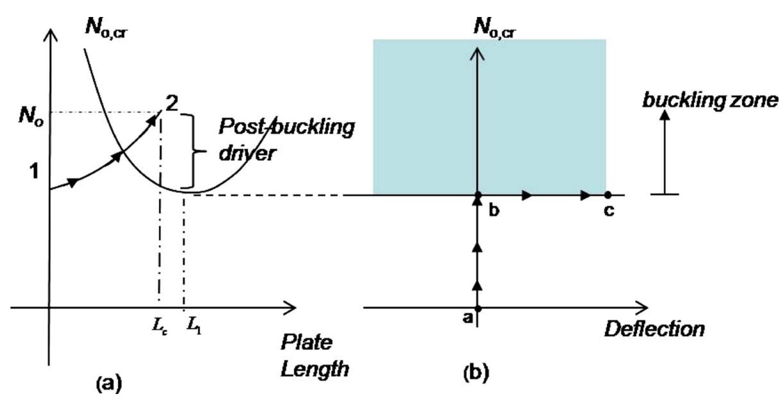

Fig. 2 The concept to determine the buckling length. (*a*) $N_{0,\mathrm{cr}}$ is the critical load calculated as a function of the plate of length. The previous approach based on the minimum critical load determines L_1 as the buckling length assuming that the axial load in the plate increases from zero while the plate length is kept constant (illustrated as the path "*a-b-c*" in Fig. 2(*b*)). (*b*) The actual path of the axial load-plate length will describe a path similar to the path illustrated as "1–2" in Fig. 2(*a*).

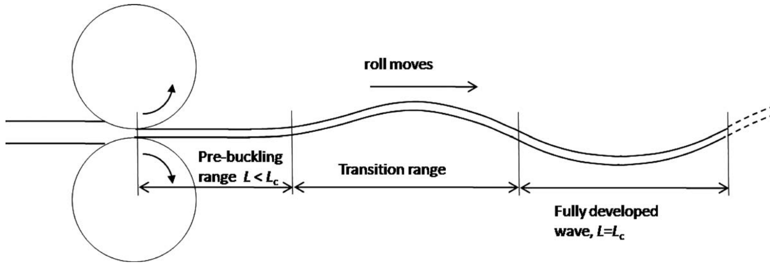

Fig. 3 Illustration to explain the process of the buckling wave formation. In the plate that keeps moving through the rollers, the length of the unbuckled part of the plate is initially very small while the axial load due to the residual stress is quite high (point 1 in Fig. 2(*a*)). As the rolling continues, this unbuckled length will increase and the axial load will also change until the load becomes large enough to cause finite buckling deflection, reaching to point 2 in Fig. 2(*a*).

enko and Gere [9], which led to an idea to develop a new method to solve the flatness problem. The strain energy of the plate subjected to an in-plane force is

$$\frac{1}{2}U = h\int_0^B \int_0^L \frac{1}{2}(\sigma_x\varepsilon_x + \sigma_y\varepsilon_y + \tau_{xy}\gamma_{xy})dxdy + \frac{1}{2}D\int_0^B \int_0^L \left\{ \left(\frac{\partial^2 w}{\partial x^2} + \frac{\partial^2 w}{\partial y^2}\right)^2 - 2(1-\nu)\left[\frac{\partial^2 w}{\partial x^2}\frac{\partial^2 w}{\partial y^2} - \left(\frac{\partial^2 w}{\partial x\,\partial y}\right)^2\right]\right\}dxdy \tag{3}$$

where $D=Eh^3/12(1-\nu^2)$ is the flexural rigidity of the plate, E is the Young's modulus, and ν is the Poisson's ratio. Notice that we consider only the upper half of the plate by taking advantage of the symmetric geometry. The stresses σ_x, σ_y, and τ_{xy} are related with strains ε_x, ε_y, and ε_{xy} as follows:

$$\sigma_x = \frac{E}{(1-\nu^2)}(\varepsilon_x + \nu\varepsilon_y), \quad \sigma_y = \frac{E}{(1-\nu^2)}(\varepsilon_y + \nu\varepsilon_x), \quad \sigma_z = 0, \quad \tau_{xy} = G\gamma_{xy}, \quad \tau_{xz} = \tau_{yz} = 0 \tag{4}$$

$$\varepsilon_x = \frac{\partial u}{\partial x} + \frac{1}{2}\left(\frac{\partial w}{\partial x}\right)^2, \quad \varepsilon_y = \frac{\partial v}{\partial y} + \frac{1}{2}\left(\frac{\partial w}{\partial y}\right)^2, \quad \gamma_{xy} = \frac{\partial v}{\partial x} + \frac{\partial u}{\partial y} + \frac{\partial w}{\partial x}\frac{\partial w}{\partial y} \tag{5}$$

The first and second integrations in Eq. (3) respectively represent the strain energies due to in-plane deflection of the midplane and the bending deflection of the plate. The total strain energy U in Eq. (3) should not be confused with the incremental strain energy used in a typical prebuckling analysis. It should be noted that w in Eq. (5) is not small, compared with h; therefore, displacements w, u, and v are all coupled.

The transverse displacement field of the plate can be assumed as follows:

$$w = W(y)\sin\frac{\pi x}{L} \tag{6}$$

where $W(y)$ represents the shape of the deflection across the width of the plate. The in-plane displacement in the x-direction is assumed as follows:

$$u = \varepsilon_o(y)\cdot\left(x - \frac{L}{2}\right) + c_u|W(y)|\sin\frac{2\pi x}{L} \tag{7}$$

where the first term represents the effect of the residual stress and the second term represents the effect of the transverse deflection due to buckling. $\varepsilon_o(y)$ is the residual strain calculated from the plasticity analysis without considering the buckling deflection. The form of the second term was chosen based on the following logics.

(1) The term should be zero valued at $x=0$ and L because the edge line should remain vertically straight after buckling to maintain the continuity of the plate.
(2) The displacement should be symmetric about the centerline ($x=0$).
(3) The magnitude of the term should be proportional to $|W(y)|$.

The in-plane displacement in the y-direction is taken as

$$v = c_v \sin\frac{\pi y}{2B}\sin\frac{\pi x}{L} \tag{8}$$

v in Eq. (8) is chosen based on following logics.

(1) v is expected to be zero at $x=0$ and L, at which w is zero, and maximum at $x=L/2$, at which w is maximum.
(2) v should be symmetric about the centerline ($y=0$).
(3) v should be maximum at the free edges ($y=B$ and $-B$), where w becomes maximum.

v is also expected to be proportional to W, however, it was not chosen as such. Because v is expected to be much smaller than u, Eq. (8) is considered to be an acceptable form. This way, v is reduced to a one-term function that simplifies the analysis considerably. A similar approach to choose the assumed displacement field is found for shell vibration analysis [12].

$W(y)$ has to be selected based on the expected form of transverse deflection. The symmetric and antisymmetric modes can be considered separately for numerical efficiency. The two-term approximation of $W(y)$ of the symmetric mode is

$$W(y) = c_1 + c_2\left(\frac{y}{B}\right)^2 \tag{9a}$$

and, of the antisymmetric mode, is

$$W(y) = c_1\left(\frac{y}{B}\right) + c_2\left(\frac{y}{B}\right)^3 \tag{9b}$$

Because $W(y)$ in the part of the plate subjected to the compression has to be larger, the antisymmetric mode is not an acceptable form for the center compression case. For example, the prebuckling analysis of the plate using Eq. (9*b*) as $W(y)$ does not yield a critical load.

The strain $\varepsilon_o(y)$ in Eq. (7) can be related to the edge load. From

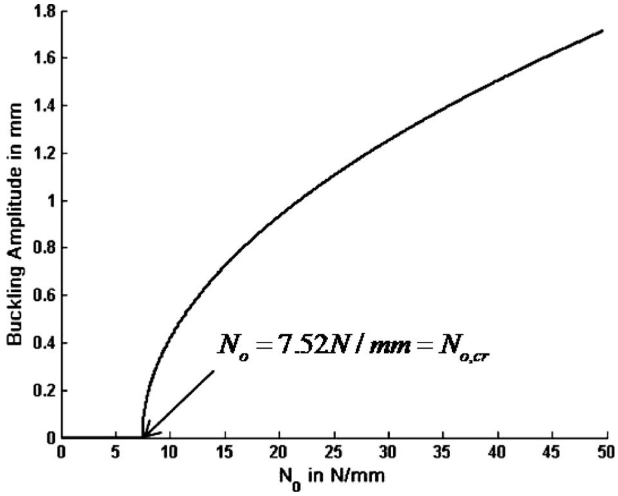

Fig. 4 Buckling amplitude as a function of the buckling load N_0

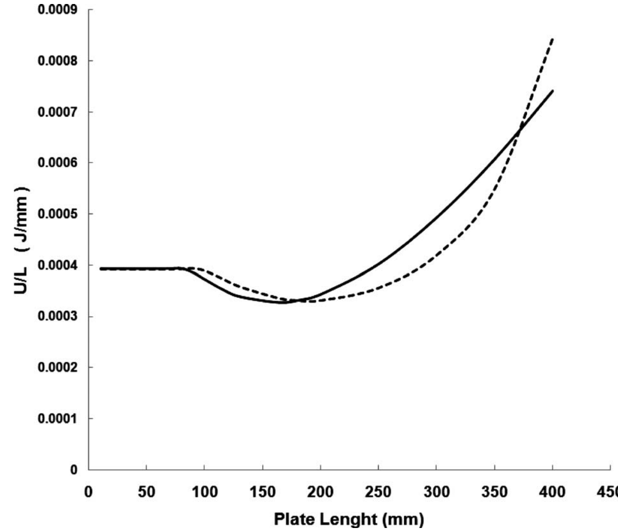

Fig. 5 Symmetric (solid line) and antisymmetric (dotted) two-term solution

Eq. (7), $\varepsilon_x=\varepsilon_o(y)$ and $\varepsilon_y=0$; therefore, $\sigma_x=N_x(y)/h=(E/1-\nu^2)\varepsilon_o(y)$ at $x=0$ and L. In the edge compression case, this leads to

$$\varepsilon_o(y) = \frac{Eh}{1-\nu^2}N_x(y) = \frac{Eh}{1-\nu^2}N_0\left[1-2\left(\frac{y}{b}\right)\right] \tag{10}$$

The center compression case can be solved by taking $\varepsilon_o(y) = -(Eh/1-\nu^2)N_x(y)$.

By substituting the assumed displacements in Eqs. (6)–(8) into Eq. (3) and performing the integration, the strain energy U is obtained as a function of c_1, c_2, c_u, c_v. The energy principle states that the deflection of the plate will take the form that minimizes the total energy of the system; therefore

$$\frac{\partial U}{\partial c_1}=0, \quad \frac{\partial U}{\partial c_2}=0, \quad \frac{\partial U}{\partial c_u}=0, \quad \frac{\partial U}{\partial c_v}=0 \tag{11}$$

Four nonlinear equations resulting from Eq. (11) are coupled. These equations have to be solved to find c_1, c_2, c_u, and c_v, which were conducted to work symbolically by using MATHEMATICA[2].

With c_1 and c_2 found, the maximum transverse deflection, i.e., the buckling amplitude, is found from Eq. (9). Figure 4 plots the buckling amplitude of the plate subjected to the edge load defined in Eq. (1) for various levels of N_0 calculated by using the symmetric buckling mode (Eq. (9*a*)). $B=200$ mm, $L=400$ mm, $h=1$ mm, and $E=229.365$ GPa were used. A nonzero buckling amplitude is obtained only when N_0 exceeds 7.52 N/mm, which is the critical load. Approximately, the same critical load is obtained by a prebuckling analysis. Obviously, the prebuckling analysis is much simpler if the critical load is the only information needed. When N_0 is lower than 7.52 N/mm, no real-valued solutions are obtained for c_1, c_2, c_u, and c_v from Eq. (11).

This energy based analysis has been used by many researchers. For example, Hutchinson [13], Xue et al. [14], and Cao and coworkers [15,16] used the critical buckling stress as the criterion to evaluate the onset of buckling.

The post-buckling process can be interpreted as follows from the energy view point.

(1) When the edge load is smaller than the critical load, the plate maintains a flat geometry because it is the configuration that gives the plate the minimum strain energy.
(2) When the edge force increases beyond the critical load, the plate takes equilibrium in a bent form because it is the geometry that gives the plate the minimum strain energy.

3 Flatness Analysis Based on Energy Method

The above-explained post-buckling analysis procedure can be extended to develop a method for the flatness analysis. It can be considered that *the wave in the plate will be formed in a way to minimize the strain energy of the entire rolled plate*.

The strain energy of the entire rolled plate is $U(L_T/L)$, where U is the strain energy of the plate of one buckling length defined in Eq. (3) (also see Fig. 1), and L_T is the total length of the rolled plate, which is typically much longer than L. L_T/L represents the number of waves in the rolled plate. To minimize the strain energy in the entire rolled plate of a given length L_T, U/L should be minimized. Therefore, the following equation should be satisfied in addition to the equations stated in Eq. (11):

$$\frac{\partial}{\partial L}\left(\frac{U}{L}\right)=0 \tag{12}$$

Solving Eqs. (11) and (12) simultaneously, the buckling length and deflection are obtained simultaneously.

Adding one nonlinear equation makes the symbolic solution of the problem considerably more difficult. As an alternative, Eq. (11) can be solved repeatedly while changing the plate length L. From the plot of U/L versus L, the buckling length can be defined as the length corresponding to the minimum U/L value. Figure 5 shows the U/L plotted as a function of L for the symmetric mode (Eq. (9*a*)) and antisymmetric mode (Eq. (9*b*)) when $B=200$ mm, $h=1$ mm, $E=229.365$ GPa, $\nu=0.25$, and $N_0=50$ N/mm. The symmetric buckling has a slightly lower minimum U/L value, therefore, it will happen in most cases. Because the difference is very small, this can also happen for antisymmetric modes with deviations of the geometry or properties of the plate products.

Figure 5 shows that the minimum U/L occurs at $L=163$ mm, which is the buckling length. It is seen that U/L value is constant when L is shorter than 78 mm. The given edge load ($N_0=50$ N/mm) is the critical load of the plate that is 78 mm long; therefore, the plate remains flat, i.e., unbuckled, for the length shorter than 78 mm.

Figure 6 is the buckling amplitude calculated for the range of L used in Fig. 7 for the symmetric mode. Theoretically, the rolled plate will buckle only with $L=163$ mm. The actual buckling length will vary slightly due to variations of the product dimen-

[2]MATHEMATICA is a product of Wolfram Research.

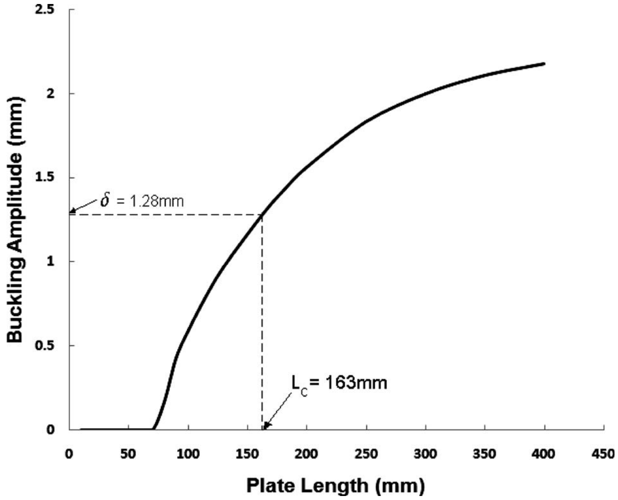

Fig. 6 Buckling amplitude obtained for a symmetric mode

sion. At this length, the buckling amplitude is 1.29 mm; therefore, the flatness (amplitude/buckling length) is predicted to be 0.79%.

4 Closed Form Solution Based on One-Term Displacement Function

Edge compression case

$$N_x(y) = N_0\left(1 - 2\left(\frac{y}{B}\right)\right)$$

$$0 \le y \le B$$

The symbolic solution of Eq. (11) becomes too lengthy to be presented in a closed form. A one-term approximation is conducted to obtain closed form solutions. To determine which term of Eq. (9) should be kept, c_1 and c_2 values are compared in Fig. 7. It is seen that two coefficients are comparable in most ranges of L in the antisymmetric case; therefore, a one-term solution will not be accurate. In the symmetric mode, c_2 is much bigger than c_1 in the entire range of L; therefore, the one-term solution can be taken for the symmetric mode as follows:

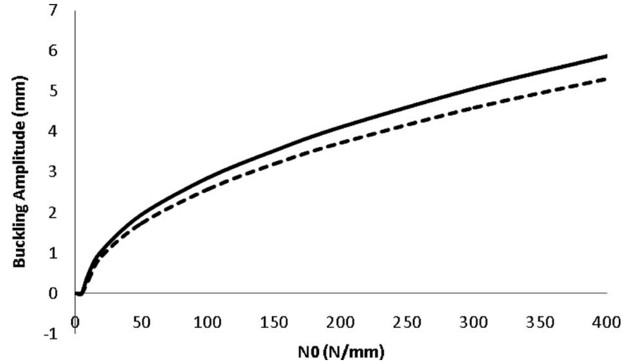

Fig. 8 Comparison of buckling amplitude calculated for the edge compression case using the symmetric mode function: one-term solution (dotted) and two-term solution (solid)

$$W(y) = c_2\left(\frac{y}{B}\right)^2 \tag{13}$$

This reduces the number of equations to solve from four to three. Figure 8 compares the buckling amplitude obtained by the one- and two-term $W(y)$ functions. The comparison confirms that the one-term solution will be a good approximation for the symmetric mode. Because the symmetric mode has a lower U/L value, the one-term solution will serve well for all cases of the edge compressed plate.

Center compression case

$$N_x(y) = N_0\left(2\left(\frac{y}{B}\right) - 1\right)$$

$$0 \le y \le B$$

As mentioned, only symmetric modes will exist in this case. c_1 and c_2 values are compared for this case in Fig. 9. The comparison indicates that neither term is negligible, compared with the other; therefore, a one-term solution will not provide a good approximation.

An alternative one-term displacement function can be considered, based on the expected deflection form of the plate as follows:

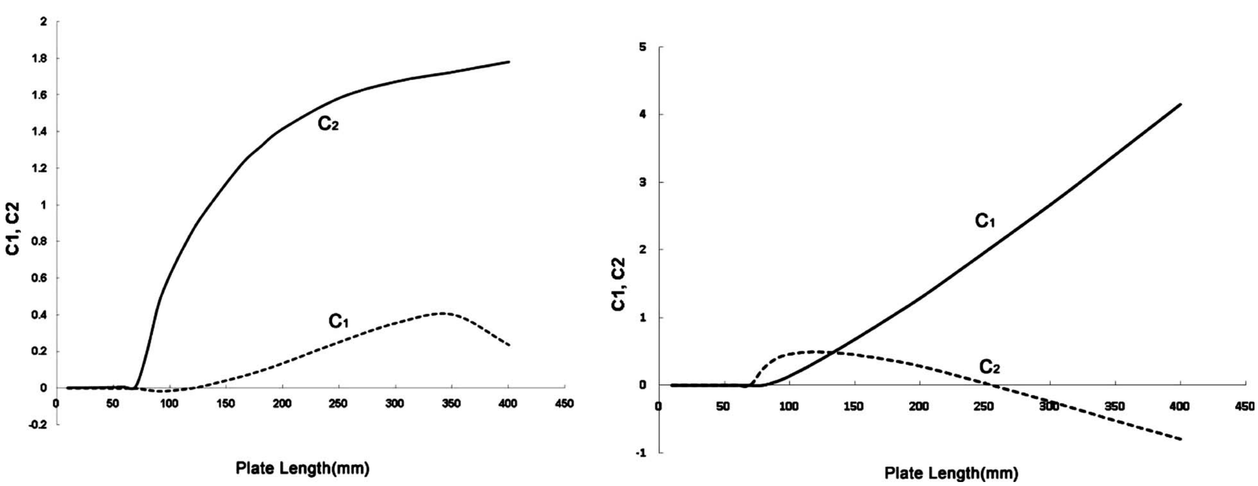

Fig. 7 Comparison of C_1 and C_2 for the edge compression case; symmetric mode (left) and antisymmetric mode (right)

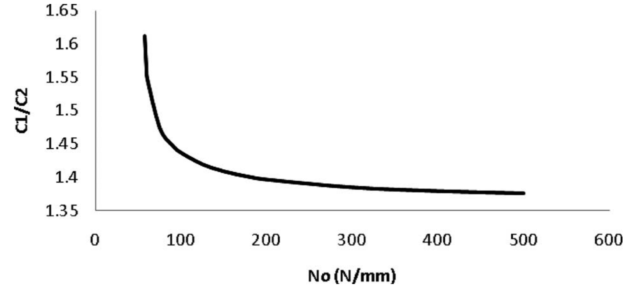

Fig. 9 Comparison of C_1 and C_2 for the center compression case

$$W(y) = c_2\left(1 - \left(\frac{y}{B}\right)^2\right) \tag{14}$$

Figure 10 compares the buckling amplitude obtained by the one-term approximation in Eq. (14) and the two-term solution obtained by using two terms (Eq. (9*a*)). The figure shows that the one-term approximation, while it is not as good as the edge buckling case, may be used for a quick, approximate estimation of the flatness. It is seen that the two-term solution provides higher amplitude, which is expected as the approximate solutions are upper-bound solutions and the two-term solution is *less* approximate than the one-term solution.

Closed form expressions of U/L and the coefficient c_2 in Eqs. (13) and (14) are shown in the Appendix for both the center compression and edge compression cases. Notice that c_2 is the maximum buckling deflection. The buckling length L is the length that corresponds to the minimum U/L. The steepness is found from the ratio of the maximum deflection and the buckling length. Being closed forms, these one-term solutions can be used for a quick estimation of the flatness.

5 Parameter Study

A parameter study was conducted to see the effects of main variables using the simulation, based on the two-term solution. Only one parameter was changed from the reference case of $B=200$ mm, $N_0=50$ N/mm, and $h=1.0$ mm. Material properties were taken as $E=229.365$ GPa, $\nu=0.275$.

Figure 11 shows the effect of the load level (N_0) on the flatness $\lambda=\delta/L$. Simulation results showed that the increase in the load decreases buckling length L while increasing the amplitude δ. As a result, flatness increases rapidly as the load increases.

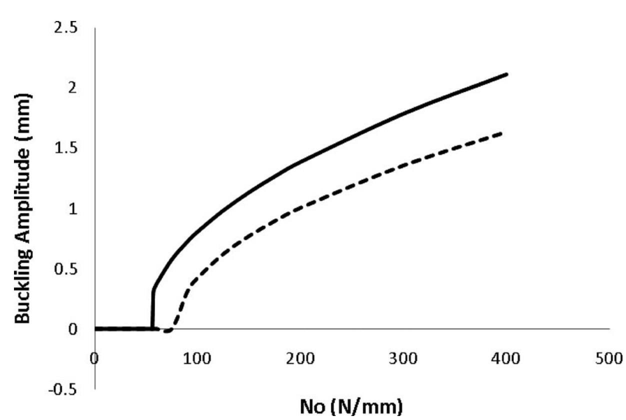

Fig. 10 Comparison of buckling amplitude calculated for the center compression case: one-term solution (dotted) and two-term solution (solid)

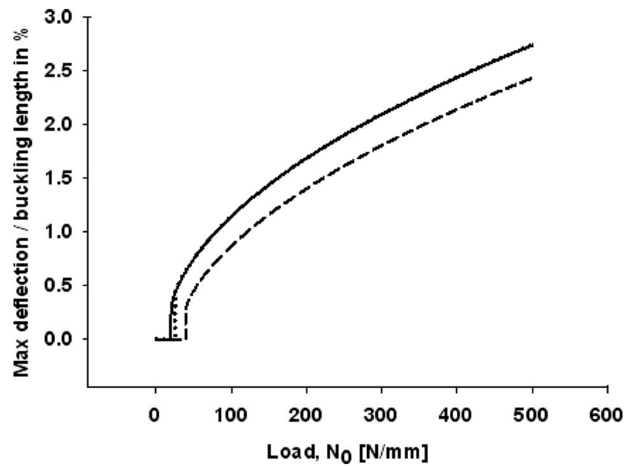

Fig. 11 Effect of magnitude of the load N_0 on flatness. Solid line: symmetric edge buckling; dotted line: antisymmetric edge buckling; dashed line: center buckling.

Figure 12 shows the effect of the plate thickness on the flatness. Simulation results showed that the increase in the thickness increases buckling length L while decreasing amplitude δ, resulting in a rapid decrease in the flatness.

Figure 13 shows that the effect of the plate width on the flatness is not significant in the range that the buckling occurs. This is because the increase in the width increases both buckling length L and buckling amplitude δ nearly at the same rate.

The observations obtained from the parameter study are not only compatible with physical insights, but also well correlated with observations in the product line [1,3].

6 Summary and Conclusion

A new analysis method has been developed to predict formation of a periodic wavy surface in a thin rolled plate. This problem, also called flatness or wave problem, is the result of post-buckling of the plate due to residual stresses formed during the rolling process. Unlike in usual buckling problems, the buckling length is not given, but has to be found in this problem. One popular approach has been to determine the buckling length as the plate length associated with the lowest critical load for the given load

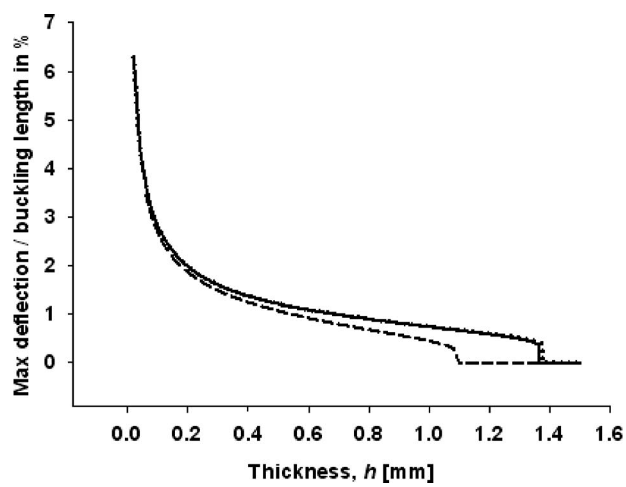

Fig. 12 Effect of the plate thickness on flatness. Solid line is symmetric edge buckling; dotted line: antisymmetric edge buckling; dashed line: center buckling.

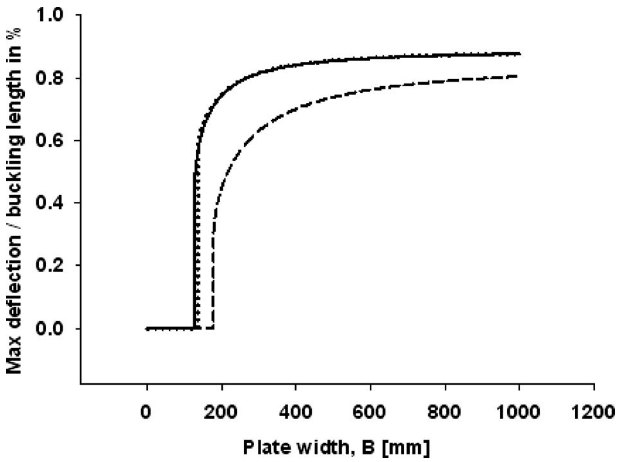

Fig. 13 Effect of the plate width on flatness. Solid line: symmetric edge buckling; dotted line: antisymmetric edge buckling; dashed line: center buckling.

profile. It is shown that the approach is actually based on a flawed interpretation of the wave formation process; therefore, it is incorrect.

The new analysis method was developed in this work by extending a classic post-buckling analysis method, based on the minimum energy principle conducted by Timoshenko and Gere [9]. The approach utilizes the fact that the buckling wave would be formed in the configuration to minimize the strain energy in the plate. Extending this interpretation, the buckling *length* could be determined from the condition to minimize the strain energy in the entire rolled plate, which minimizes the strain energy per unit length of the plate. This new approach enables solving this type of post-buckling problem correctly for the first time without using any unfounded assumption or hypothesis. Analytic solutions, based on two-term displacement functions and one-term displacement functions, were obtained. Especially, the one-term solutions were obtained in closed forms, which can be used for the quick prediction of formation of the buckling wave.

The new approach can be implemented with any numerical method including the finite element method (FEM). For example, FEM based post-buckling solutions can be obtained repeatedly while varying the length of the plate; then the result that corresponds to the minimum U/L can be taken as the solution. A semi-analytic solution procedure of the approach can also be developed. A Newton–Rhapson method based approach is being developed, which will be reported very soon in a sequel paper. Numerical methods can solve flatness problems subjected to more general forms of edge load.

The correct analysis method to solve the flatness problem has a significant commercial value. Along with a rolling simulation program that calculates the residual stress available, the developed method can determine the rolling condition for the maximum productivity without incurring the flatness problem. The procedure is envisioned as follows.

(1) Estimate the residual stress by using a rolling simulation program for the given production speed.
(2) Calculate the predicted flatness by using the developed analysis method.
(3) If the flatness exceeds the maximum allowed, the residual stress will have to be decreased, which will require more gradual reduction in thickness, therefore, more rolling stations; if the flatness is significantly smaller than the maximum allowed, more rapid reduction in thickness, i.e., fewer rolling stations can be used. This will enable a higher throughput of the given rolling system.

It is noted that the developed analysis procedure still relies on many simplifications as it ignores various effects such as chattering of the roll system, temperature changes, friction, and nonlinearity of material properties. Effects of these simplifications will have to be the subjects of future research.

Acknowledgment

Financial support by POSTECH for this work is highly appreciated.

Appendix: Closed Form One-Term Solution

- U/L is the strain energy of the plate per unit length. By plotting U/L, the length that corresponds to the minimum value of U/L is identified as the buckling length.
- C_2 is the coefficients in Eqs. (13) and (14). C_2 is actually the maximum buckling amplitude.
- The same definitions of variables are used; for example, B is the plate width, L is the plate length, h is the plate thickness, E is the Young's modulus, and N_0 is the load. "a, b, c, d" were used to make the equations more tractable.

Edge compression case

$$N_x(y) = N_0\left(1 - 2\left(\frac{y}{B}\right)\right)$$

Symmetric mode

$$W(y) = C_2\left(\frac{y}{B}\right)^2$$

$$U/L(C_2,L,B,h,E) = \frac{a}{b}$$

$$\begin{aligned} a = {} & (B^2N_0^2L^4(2.085B^{18} + 8.83L^2B^{16} + 15.8L^4B^{14} + 15.57L^6B^{12} \\ & + 9.03L^8B^{10} + 3.096L^{10}B^8 + 0.59L^{12}B^6 + 0.0568L^{14}B^4 \\ & + 0.002563L^{16}B^2 + 4.3 \times 10^{-5}L^{18}) + B^2C_2^2hEN_0L^2(-0.954B^{18} \\ & - 4.0798L^2B^{16} - 7.404L^4B^{14} - 7.38L^6B^{12} - 4.38L^8B^{10} \\ & - 1.55L^{10}B^8 0.317L^{12}B^6 - 0.034L^{14}B^4 - 1.78 \times 10^{-3}L^{16}B^2 \\ & - 3.58 \times 10^{-5}L^{18}) + C_2^2h^2((0.736C_2^2 + 0.849h^2)B^{20} + (3.35C_2^2 \\ & + 4.42h^2)L^2B^{18} + (6.85C_2^2 + 9.321h^2)L^4B^{16} + (8.35C_2^2 \\ & + 11.82h^2)L^6B^{14} + (6.83C_2^2 + 9.53h^2)L^8B^{12} + (3.93C_2^2 \\ & + 5.05h^2)L^{10}B^{10} + (1.58C_2^2 + 1.76h^2)L^{12}B^8(0.418C_2^2 \\ & + 0.389h^2)L^{14}B^6 + (0.064C_2^2 + 0.049h^2)L^{16}B^4 + (4.42 \\ & \times 10^{-3}C_2^2 + 3.08 \times 10^{-3}h^2)L^{18}B^2 + (1.08 \times 10^{-4}C_2^2 + 7.02 \\ & \times 10^{-5}h^2)L^{20}) \end{aligned}$$

$$b = B^3h^2L^4E^2(B^8 + 2.1L^2B^6 + 1.512L^4B^4 + 0.401L^6B^2 + 0.02L^8)^2$$

$C_2 = \sqrt{c/d}$, which is the maximum buckling deflection, where

$$\begin{aligned} c = {} & N_0B^2L^2(1.91B^{18} + 8.15L^2B^{16} + 14.8L^4B^{14} + 14.77L^6B^{12} \\ & + 8.768L^8B^{10} + 3.117L^{10}B^8 + 0.635L^{12}B^6 + 0.068L^{14}B^4 + 3.56 \\ & \times 10^{-3}L^{16}B^2 + 7.1 \times 10^{-5}8L^{18} - h^3E(1.69B^{20} + 8.482L^2B^{18} \\ & + 18.64L^4B^{16} + 23.64L^6B^{14} + 19.06L^8B^{12} + 10.11L^{10}B^{10} \\ & + 3.527L^{12}B^8 + 0.779L^{14}B^6 + 0.099L^{16}B^4 + 6.16 \times 10^{-3}L^{18}B^2 \\ & + 1.4 \times 10^{-4}L^{20} \end{aligned}$$

$$d = hE(2.945B^{20} + 13.429L^2B^{18} + 27.412L^4B^{16} + 33.433L^6B^{14} + 27.349L^8B^{12} + 15.733L^{10}B^{10} + 6.327L^{12}B^8 + 1.674L^{14}B^6 + 0.256L^{16}B^4 + 0.0177L^{18}B^2 + 4.35 \times 10^{-4}L^{20})$$

Center compression case

$$N_x(y) = N_0\left(2\left(\frac{y}{B}\right) - 1\right)$$

Symmetric mode

$$W(y) = C_2\left(1 - \left(\frac{y}{B}\right)^2\right)$$

$$U/L(C_2,L,B,h,E) = \frac{a}{b}$$

$$\begin{aligned} a = {} & (B^2N_0^2L^4(4137.7B^{18} + 16774.1L^2B^{16} + 29471.3L^4B^{14} \\ & + 29431.L^6B^{12} + 18324.9L^8B^{10} + 7250.58L^{10}B^8 + 1732.2L^{12}B^6 \\ & + 207.901L^{14}B^4 + 6.06246L^{16}B^2 + 0.0462677L^{18}) \\ & + B^2C_2^2hEN_0L^2(-13253.5B^{18} - 49771.2L^2B^{16} - 74248L^4B^{14} \\ & - 52970.8L^6B^{12} - 14479.7L^8B^{10} + 3185.92L^{10}B^8 \\ & + 2968.87L^{12}B^6 + 582.509L^{14}B^4 + 20.1868L^{16}B^2 \\ & + 0.186186L^{18}) + C_2^2h^2((36580.5C_2^2 + 31446.4h^2)B^{20} \\ & + (151672C_2^2 + 144327h^2)L^2B^{18} + (268469C_2^2 \\ & + 286882h^2)L^4B^{16} + (266026C_2^2 + 322599h^2)L^6B^{14} \\ & + (164157C_2^2 + 224781h^2)L^8B^{12} + (67598.9C_2^2 \\ & + 99830.2h^2)L^{10}B^{10} + (19785.5C_2^2 \\ & + 27941.4h^2)L^{12}B^8(4147.96C_2^2 + 4669.15h^2)L^{14}B^6 \\ & + (515.777C_2^2 + 408.446h^2)L^{16}B^4 + (19.0894C_2^2 \\ & + 13.1836h^2)L^{18}B^2 + (0.212577C_2^2 + 0.137278h^2)L^{20}) \end{aligned}$$

$$b = 14527.3B^3h^2L^4E^2(B^8 + 2.04151L^2B^6 + 1.40483L^4B^4 + 0.336794L^6B^2 + 0.007529L^8)^2$$

$C_2 = \sqrt{c/d}$, where

$$\begin{aligned} c = {} & N_0B^2L^2(26507.1B^{18} + 99542.5L^2B^{16} + 148496.L^4B^{14} \\ & + 105942L^6B^{12} + 28959.4L^8B^{10} - 6371.84L^{10}B^8 \\ & - 5937.73L^{12}B^6 - 1165.02L^{14}B^4 - 40.3736L^{16}B^2 \\ & - 0.372373L^{18} - h^3E(62892.7B^{20} + 288654L^2B^{18} \\ & + 573764L^4B^{16} + 645198L^6B^{14} + 449562L^8B^{12} \\ & + 199660L^{10}B^{10} + 55882.9L^{12}B^8 + 9338.3L^{14}B^6 \\ & + 816.892L^{16}B^4 + 26.36L^{18}B^2 + 0.2745L^{20} \end{aligned}$$

$$\begin{aligned} d = {} & hE(146322B^{20} + 606687L^2B^{18} + 1.07388 \times 10^6L^4B^{16} + 1.0641 \\ & \times 10^6L^6B^{14} + 656627L^8B^{12} + 270396L^{10}B^{10} + 79142.L^{12}B^8 \\ & + 16591.9L^{14}B^6 + 2063.11L^{16}B^4 + 76.3575L^{18}B^2 + 0.85L^{20}) \end{aligned}$$

References

[1] Ginzburg, V. B., and Ballas, R., 2000, *Flat Rolling Fundamentals*, Dekker, New York, pp. 439–460.

[2] Ginzburg, V. B., and Ballas, R., 1993, *High-Quality Steel Rolling—Theory and Practice*, Dekker, New York, pp. 3–28.

[3] Shohet, K. N., and Townsend, N. A., 1971, "Flatness Control in Plate Rolling," J. Iron Steel Inst., London, **11**, pp. 769–775.

[4] Rammerstorfer, F. G., Fischer, F. D., and Friedl, N., 2001, "Buckling of Free Infinite Strips Under Residual Stresses and Global Tension," ASME J. Appl. Mech., **68**, pp. 399–404.

[5] Fischer, F. D., Rammersdorfer, F. G., Friedel, N., and Wieser, W., 2000, "Buckling Phenomenon Related to Rolling and Leveling of Sheet Metal," Int. J. Mech. Sci., **42**, pp. 1887–1910.

[6] Zhou, Z., Lam, Y. C., Thompson, P. F., and Yuen, D. D., 2007, "Numerical Analysis of the Flatness of Thin, Rolled Steel Strip on the Runout Table," Proc. Inst. Mech. Eng., Part B, **221**, pp. 241–254.

[7] Komori, K., 1998, "Analysis of Cross and Longitudinal Buckle in Sheet Metal Rolling," Int. J. Mech. Sci., **40**, pp. 1235–1246.

[8] Yoshida, H., 1984, "Analysis of Flatness of Hot Rolled Steel Strip After Cooling," Trans. Iron Steel Inst. Jpn., **24**, pp. 212–220.

[9] Timoshenko, S. P., and Gere, J. M., 1963, *Theory of Elastic Stability*, McGraw-Hill, New York.

[10] Kim, Y. K., and Hwang, S. M., 2004, *Roll Force and Tension Distribution Along the Width for the Precision Prediction of Strip Deformation*, The Korean Society for Technology of Plasticity, Seoul, Korea, pp. 153–162.

[11] Reddy, J. N., 1992, *Energy and Variational Methods in Applied Mechanics*, Wiley, New York, pp. 121–139, 183–211, 332–336.

[12] Soedel, W., 2004, *Vibration of Shells and Plates*, 3rd ed., Dekker, New York.

[13] Hutchinson, J. W., 1974, "Plastic Buckling," Adv. Appl. Mech., **14**, pp. 67–144.

[14] Xue, P., Yu, T. X., and Chu, E., 2001, "An Energy Approach for Predicting Springback of Metal Sheets After Double-Curvature Forming—Part I: Axisymmetric Stamping," Int. J. Mech. Sci., **43**, pp. 1893–1914.

[15] Cao, J., and Wang, X., 2000, "An Analytical Model for Plate Wrinkling Under Tri-Axial Loading and Its Application," Int. J. Mech. Sci., **42**, pp. 617–633.

[16] Cao, J., Karafillis, A., and Ostrowski, M., 1997, "Prediction of Flange Wrinkles in Deep Drawing," Studies in Applied Mechanics, **45**, pp. 301–310.